A comparative study of Heisenberg-like models with and without internal spin fluctuations

1997 J. Phys.: Condens. Matter 9 5643

(http://iopscience.iop.org/0953-8984/9/26/012)

J. Phys.: Condens. Matter **9** (1997) 5643–5653. Printed in the UK PII: S0953-8984(97)79475-X

A comparative study of Heisenberg-like models with and without internal spin fluctuations

Ke Xia, Weiyi Zhang, Mu Lu and Hongru Zhai

National Laboratory of Solid State Microstructures and Department of Physics, Nanjing University, Nanjing 210093, People's Republic of China

Received 12 November 1996, in final form 8 January 1997

Abstract. A comparative study has been carried out on the magnetic properties of the Heisenberg-like models with and without internal spin fluctuations. A two-spins-per-site Heisenberg-like model is used to mimic the internal spin fluctuations inside atoms. Using the double-time Green's function decoupling method, we have calculated the magnetization and paramagnetic susceptibility of the model Hamiltonians for different atomic spins as functions of the temperature and exchange energies. Our study suggests that the internal spin fluctuations generally reduce the transition temperature, and modify the magnetic behaviours. Unlike the results obtained by using the usual Heisenberg model, our results show that the Curie constant of the two-spins-per-site Heisenberg model depends on the individual moments, rather than on the resultant saturated magnetic moment. The possible physical implication of our result is also discussed.

1. Introduction

The Heisenberg Hamiltonian [1] has been studied extensively in the past [2–10]: its magnetic behaviour above the Curie temperature T_C was studied using the high-temperature expansion method [2, 3], the low-temperature properties were investigated by the spin-wave method [4], and the Green's function decoupling technique [5, 6] was employed to give a unified magnetic picture over the whole temperature range. All of these studies have shown that the paramagnetic susceptibility $\chi(T)$ above T_C satisfies the Curie–Weiss law, and can be expressed as $\chi = C/(T - T_C)$, where $C = \mu_{eff}^2/3k_B$ is the Curie constant. In the absence of internal spin fluctuations, μ_{eff} is also the saturated magnetic moment. However, this relationship between the Curie constant and the saturated magnetic moment is established on the assumption that the total atomic spin magnitude is fixed, and no internal spin fluctuations inside the atom are possible.

In practice, the atomic spin in the transition metal oxides is contributed by the electronic spins in the different orbitals; thus the total atomic spin is not fixed, and spin fluctuations inside the atom are unavoidable. For the transition metal oxides, the crystal field splits the five d orbitals into the degenerate doublet e_g levels and triplet t_{2g} levels. This may suggest that the total atomic spin is composed of two sub-spins $\boldsymbol{S}^d$ and $\boldsymbol{S}^t$ contributed by the doublet and triplet states, respectively. We assume that the spin fluctuations inside the degenerate orbitals e_g or t_{2g} are small, and that orientation fluctuations among the $\boldsymbol{S}^d$ and $\boldsymbol{S}^t$ can be large. In this way, we hope to simulate some of the magnitude fluctuation of the atomic spin. Thus, we extend the usual one-spin-per-site Heisenberg model to the two-spins-per-site situation. The relative orientations of the two sub-spins imitate the internal

0953-8984/97/265643+11$19.50

spin fluctuations. In fact, this model is also closely related to the binary magnetic alloy system, where the two sub-spins represent the two atomic spins in the cell. To find out how the internal spin fluctuations affect the magnetic properties of this two-spins-per-site Heisenberg model, it is of interest to make a comparative study of the magnetic properties of the two-spins-per-site and the one-spin-per-site models for the whole temperature range. Physically speaking, the spontaneous magnetization below the critical temperature depends sensitively on the total atomic spin or the saturated magnetic moment of the atom, while the paramagnetic susceptibility above the critical temperature depends instead on the sub-spins, because of the thermal fluctuations.

In this paper, we have studied the magnetization and paramagnetic susceptibility of the two-spin Heisenberg model for various values of sub-spins, using the conventional Green's function decoupling technique. Our results show that the magnetization as a function of temperature depends strongly on all of the inter-atomic exchange energies, while the Curie temperature is determined by the largest exchange energy of neighbouring sub-spins of the same species, and the effective atomic spin. In contrast to the results obtained by using the one-spin-per-site Heisenberg Hamiltonian, where the Curie constant depends on the resultant saturated magnetic moment, our results show that the Curie constant of the two-spins-per-site Heisenberg model depends instead on the individual moments. Thus, in the case of large internal spin fluctuations within an atom, there is no direct connection between the saturated magnetization $M(T=0)$ and the Curie constant C.

We would like to mention here that various modifications of the Heisenberg model and its extensions have been proposed previously. For example, motivated by the Van Vleck argument [11] that the intra-atomic exchange interaction plays an important role in the transition metal ferromagnetism, Inagaki [12] and Takano and Uchinami [13] formulated a model for the doubly degenerate d-orbital states with one electron per atom. The spin and isospin operators for the orbital degree were used in their model, and their averages are taken as order parameters. An analysis of this spin–isospin Heisenberg model was carried out in the molecular-field approximation, and two phase transitions were observed. The phase diagram of this model was also studied by Kugel and Khomskii [14], and the exact solution for the one-dimensional chain and for the symmetry interaction was obtained by Uimin [15]. Note that this model is different from our model, in which the two spins do represent the spin degree of freedom.

The rest of the paper is organized as follows. In section 2, the model Hamiltonian is presented, the solution of the problem is formulated in terms of the Green's function decoupling method, and a set of self-consistent equations are derived. The numerical results of our calculations of the magnetization and inverse paramagnetic susceptibility are given and discussed in section 3. Section 4 gives our conclusions.

2. The model Hamiltonian and its solution

The two-spins-per-site Heisenberg model which imitates the internal spin fluctuation has the following Hamiltonian:

$$\mathcal{H} = -g\mu_B \boldsymbol{H}_{ext} \cdot \sum_i (\boldsymbol{S}_i^d + \boldsymbol{S}_i^t) - \frac{1}{2}\sum_{i,\delta} (\,\boldsymbol{S}_i^d \quad \boldsymbol{S}_i^t\,) \begin{pmatrix} J_1 & J_3 \\ J_3 & J_2 \end{pmatrix} \begin{pmatrix} \boldsymbol{S}_{i+\delta}^d \\ \boldsymbol{S}_{i+\delta}^t \end{pmatrix} - \frac{1}{2}\sum_i (\,\boldsymbol{S}_i^d \quad \boldsymbol{S}_i^t\,) \begin{pmatrix} 0 & J_0 \\ J_0 & 0 \end{pmatrix} \begin{pmatrix} \boldsymbol{S}_i^d \\ \boldsymbol{S}_i^t \end{pmatrix}. \tag{1}$$

Here, $\boldsymbol{S}^d$ and $\boldsymbol{S}^t$ stand for the two spin operators of the system. $\boldsymbol{H}_{ext}$ refers to external field, g is Landé factor, and μ_B is the Bohr magneton. i is the lattice site index, and δ denotes the nearest neighbour of site i. J_0 is the intra-site spin exchange energy, which favours on-site parallel alignment of the two spins when it is positive, and vice versa. J_1, J_2, and J_3 are the inter-site spin exchange energies, which impose conditions on the alignment of the neighbouring spins. Unlike in the one-spin-per-site Heisenberg model, where the system is either ferromagnetic or antiferromagnetic depending on the sign of the exchange energy J, the extended two-spin model can even have states where one spin species has ferromagnetic coupling and the other spin species has antiferromagnetic coupling. In the following, we restrict ourselves to the case of the ferromagnetic state.

According to the Green's function decoupling method, the problem of obtaining the magnetic properties of the model Hamiltonian amounts to solving the retarded Green's functions as defined below:

$$\begin{aligned} G_{ij}^{\alpha\beta(n)}(t-t') &= \langle\langle S_i^{\alpha+}(t); (S_j^{\beta-}(t'))^n (S_j^{\beta+}(t'))^{n-1}\rangle\rangle \\ &= -\mathrm{i}\theta(t-t')\langle[S_i^{\alpha+}(t); (S_j^{\beta-}(t'))^n (S_j^{\beta+}(t'))^{n-1}]\rangle. \end{aligned} \tag{2}$$

$(\alpha, \beta) = (d, t)$, $S^{\pm} = S^x \pm \mathrm{i}S^y$ are the raising and lowering operators, $\theta(t)$ is the step function of time, and $\langle\ \rangle$ denotes the thermal average. $[A, B]$ stands for the commutator of the operators A and B. The integer n takes the values $1, 2, \ldots, 2S^d$ for $G_{ij}^{dd(n)}(t-t')$ and $G_{ij}^{dt(n)}(t-t')$, and $1, 2, \ldots, 2S^t$ for $G_{ij}^{td(n)}(t-t')$ and $G_{ij}^{tt(n)}(t-t')$, respectively. The required Green's functions in the frequency and momentum space, $G_{\boldsymbol{k}}^{dd(n)}(\omega)$ and $G_{\boldsymbol{k}}^{tt(n)}(\omega)$, are given by

$$G_{\boldsymbol{k}}^{dd(n)}(\omega) = \frac{\langle[S^{d+}, (S^{d-})^n (S^{d+})^{n-1}]\rangle(\omega - E_{\boldsymbol{k}2})}{(\omega - E_{\boldsymbol{k}1})(\omega - E_{\boldsymbol{k}2}) - \left[J_0 + J_3\gamma(\boldsymbol{k})\right]^2 \langle S^{dz}\rangle\langle S^{tz}\rangle} \tag{3a}$$

$$G_{\boldsymbol{k}}^{tt(n)}(\omega) = \frac{\langle[S^{t+}, (S^{t-})^n (S^{t+})^{n-1}]\rangle(\omega - E_{\boldsymbol{k}1})}{(\omega - E_{\boldsymbol{k}1})(\omega - E_{\boldsymbol{k}2}) - \left[J_0 + J_3\gamma(\boldsymbol{k})\right]^2 \langle S^{dz}\rangle\langle S^{tz}\rangle} \tag{3b}$$

with

$$E_{\boldsymbol{k}1} = g\mu_B H_{ext} + J_1(\gamma(0) - \gamma(\boldsymbol{k}))\langle S^{dz}\rangle + (J_0 + J_3\gamma(0))\langle S^{tz}\rangle \tag{4a}$$

$$E_{\boldsymbol{k}2} = g\mu_B H_{ext} + J_2(\gamma(0) - \gamma(\boldsymbol{k}))\langle S^{tz}\rangle + (J_0 + J_3\gamma(0))\langle S^{dz}\rangle. \tag{4b}$$

$\gamma(\boldsymbol{k}) \equiv \sum_{\boldsymbol{R}_\delta} \mathrm{e}^{\mathrm{i}\boldsymbol{k}\cdot\boldsymbol{R}_\delta}$ is the structure factor. Then the self-consistent equations determining $\langle S^{dz}\rangle$ and $\langle S^{tz}\rangle$ are easily obtained from the spectrum theorem:

$$\langle S^{dz}\rangle = \begin{cases} \dfrac{1}{2(1+2\Phi_1)} & (S^d = \frac{1}{2}) \\ \dfrac{1+2\Phi_1}{1+3\Phi_1+3\Phi_1^2} & (S^d = 1) \\ \dfrac{\frac{3}{2}+5\Phi_1+5\Phi_1^2}{(1+\Phi_1)^4 - \Phi_1^4} & (S^d = \frac{3}{2}) \end{cases} \tag{5a}$$

$$\langle S^{tz}\rangle = \begin{cases} \dfrac{1}{2(1+2\Phi_2)} & (S^t = \frac{1}{2}) \\ \dfrac{1+2\Phi_2}{1+3\Phi_2+3\Phi_2^2} & (S^t = 1) \end{cases} \tag{5b}$$

where

$$\Phi_1 = \frac{1}{N}\sum_{\boldsymbol{k}} \frac{1}{E_{\boldsymbol{k}+} - E_{\boldsymbol{k}-}} \left[\frac{E_{\boldsymbol{k}+} - E_{k2}}{\mathrm{e}^{\beta E_{\boldsymbol{k}+}} - 1} - \frac{E_{\boldsymbol{k}-} - E_{k2}}{\mathrm{e}^{\beta E_{\boldsymbol{k}-}} - 1} \right] \tag{6a}$$

$$\Phi_2 = \frac{1}{N}\sum_{\boldsymbol{k}} \frac{1}{E_{\boldsymbol{k}+} - E_{\boldsymbol{k}-}} \left[\frac{E_{\boldsymbol{k}+} - E_{k1}}{\mathrm{e}^{\beta E_{\boldsymbol{k}+}} - 1} - \frac{E_{\boldsymbol{k}-} - E_{k1}}{\mathrm{e}^{\beta E_{\boldsymbol{k}-}} - 1} \right] \tag{6b}$$

and

$$E_{\boldsymbol{k}\pm} = \frac{(E_{k1} + E_{k2}) \pm \sqrt{(E_{k1} - E_{k2})^2 + 4(J_0 + J_3\gamma(\boldsymbol{k}))^2\langle S^{dz}\rangle\langle S^{tz}\rangle}}{2}. \tag{7}$$

$\beta = 1/k_B T$ is the inverse temperature. Equations (5)–(7) form a closed set for computing the equilibrium magnetization for both the individual spin species and their summation.

3. Numerical results and discussion

We have studied the magnetic properties of the model Hamiltonian for different atomic spins as functions of the temperature and exchange energies, and these results are compared with those obtained by using the usual Heisenberg model. For the numerical calculation, we have restricted ourselves to a three-dimensional cubic lattice. In this case, the structural factor $\gamma(\boldsymbol{k}) = 2(\cos(k_x a) + \cos(k_y a) + \cos(k_z a))$, where a is the lattice constant. The equilibrium values of $\langle S^{dz}\rangle$ and $\langle S^{tz}\rangle$ are calculated by the iteration method. Since it is difficult to obtain an analytical expression for the magnetic susceptibility, we calculate the magnetization for small external magnetic fields numerically and get the magnetic susceptibility from its slope. Our detailed numerical calculations show that the magnetic structure depends sensitively on the magnetic interactions present in the model. While the parameters J_1 and J_2 control the neighbouring sub-spin alignments for $\boldsymbol{S}^d$ and $\boldsymbol{S}^t$, respectively, J_0 and J_3 determine the relative orientations of the two sub-spin species. In the case of weak couplings of the two sub-spin species, the Curie temperature is mainly determined by the sub-spin species which has the largest inter-atomic exchange energy. While the saturated magnetic moment at zero temperature is given by $S^{dz} + S^{tz}$ when J_0 and J_3 favour the parallel alignment, the Curie constant deduced from the high-temperature paramagnetic susceptibility does not depend on the total saturated moment; instead it depends on the sub-spin moments and can be nicely expressed as $C \propto [S^d(S^d+1) + S^t(S^t+1)]/3k_B$. Thus, even if the total saturated magnetic moment is large, the Curie temperature can be low when J_3 and J_0 are small, and thus so can the Curie constant.

To study the effect of the internal spin fluctuations on the magnetic properties of the two-spins-per-site Heisenberg model, we first calculate the magnetization and paramagnetic susceptibility of our model with the sub-spins $S^d = 1$, $S^t = 1/2$, and compare them with those obtained by using the usual Heisenberg model with $S = 3/2$ and $J = J_1$. As we can see from equation (1), our model resembles the usual Heisenberg model when all of the inter-atomic exchange energies J_1, J_2, and J_3 take the same values. Thus, in the following, we set $J_1 = 1$, and discuss the role played by J_0, J_2, and J_3, separately.

In figures 1(a) and 1(b), the temperature-dependent magnetization $M(T) = g\mu_B(S^{dz} + S^{tz})$ and the paramagnetic susceptibility $\chi(T) = \partial M/\partial H$ are shown for various values of J_2, while the other parameters are fixed at $J_1 = 1.0$, $J_0 = 0$, and $J_3 = 0.25$. The motivation is to see how the imbalance of the two sub-spin systems affects the total magnetization as well as the paramagnetic susceptibility. The dotted, dashed, chain–dotted, and chain–double-dotted lines refer to $J_2 = -0.1,\ 0.1,\ 0.5,\ 1.0$, respectively. The solid line refers to the usual Heisenberg model. As we can see from figure 1(a), the saturated magnetic moments

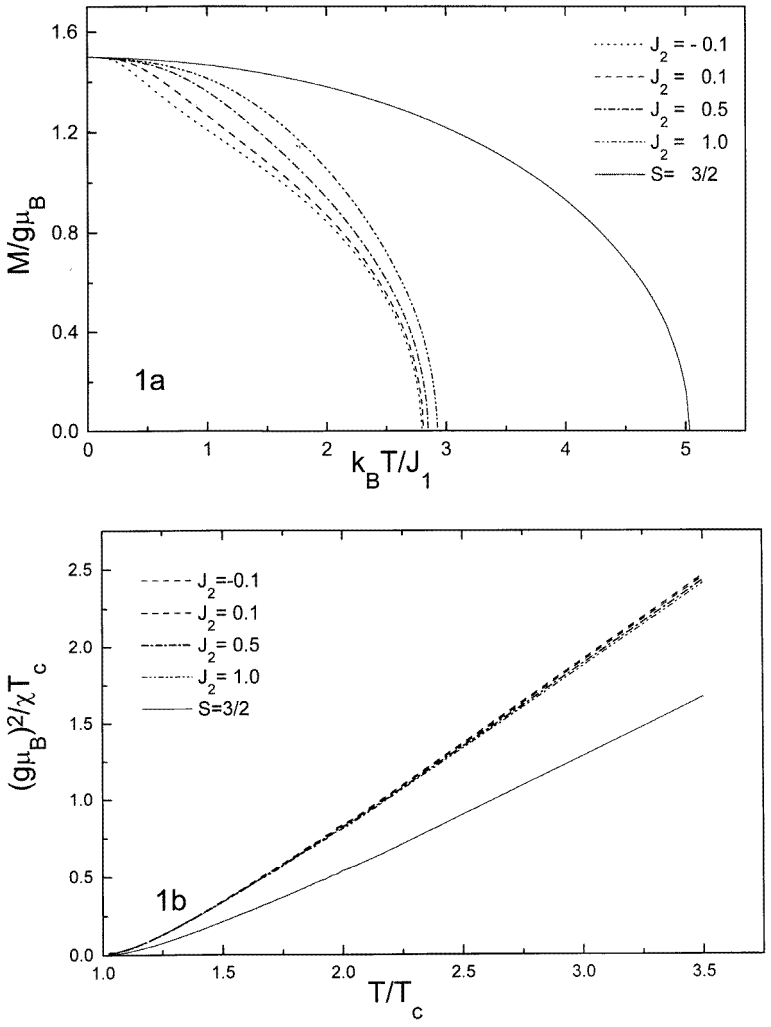

Figure 1. (a) The magnetization and (b) inverse paramagnetic susceptibility as functions of the temperature and J_2. The other parameters are $J_1 = 1.0$, $J_0 = 0$, and $J_3 = 0.25$. The dotted, dashed, chain–dotted, and chain–double-dotted lines refer to $J_2 = -0.1,\ 0.1,\ 0.5,\ 1.0$, respectively. The solid line corresponds to the usual Heisenberg model, with $S = 3/2$ and $J = 1$.

are the same for the two-spins-per-site and the usual one-spin-per-site Heisenberg models. When temperature increases, the magnetization curve of the two-spins-per-site model starts to deviate from that of the usual Heisenberg model, and the change is most significant when the two sub-spin species become most asymmetrical. The Curie temperatures deduced are $k_BT_C/J_1 = 2.80,\ 2.81,\ 2.85,\ 2.93$ for $J_2 = -0.1,\ 0.1,\ 0.5,\ 1.0$, respectively. The Curie temperature for the usual Heisenberg model is $k_BT_C/J = 5.03$, which agrees with the previous result. The magnetization curve with $J_2 = 1$ does not approach the one for the usual Heisenberg model because of the small value that we take for $J_3 = 0.25$. In this case, the two sub-spin species are not tightly bound together, and strong internal spin fluctuations decrease the effective total atomic spin, and thus the Curie temperature.

The inverse paramagnetic susceptibility of our model above the Curie temperature is shown in figure 1(b) as a function of reduced temperature for the same set of values of J_2; the slopes at high temperature are almost independent of the exchange energies. This is so since the two sub-spin species are thermally decoupled from each other at high temperature, and their contributions to the paramagnetic susceptibility are additive and given by $C \propto [S^d(S^d+1) + S^t(S^t+1)]/3k_B$. Note that the slope of the paramagnetic susceptibility of the usual Heisenberg model is given by $C \propto S(S+1)/3k_B$.

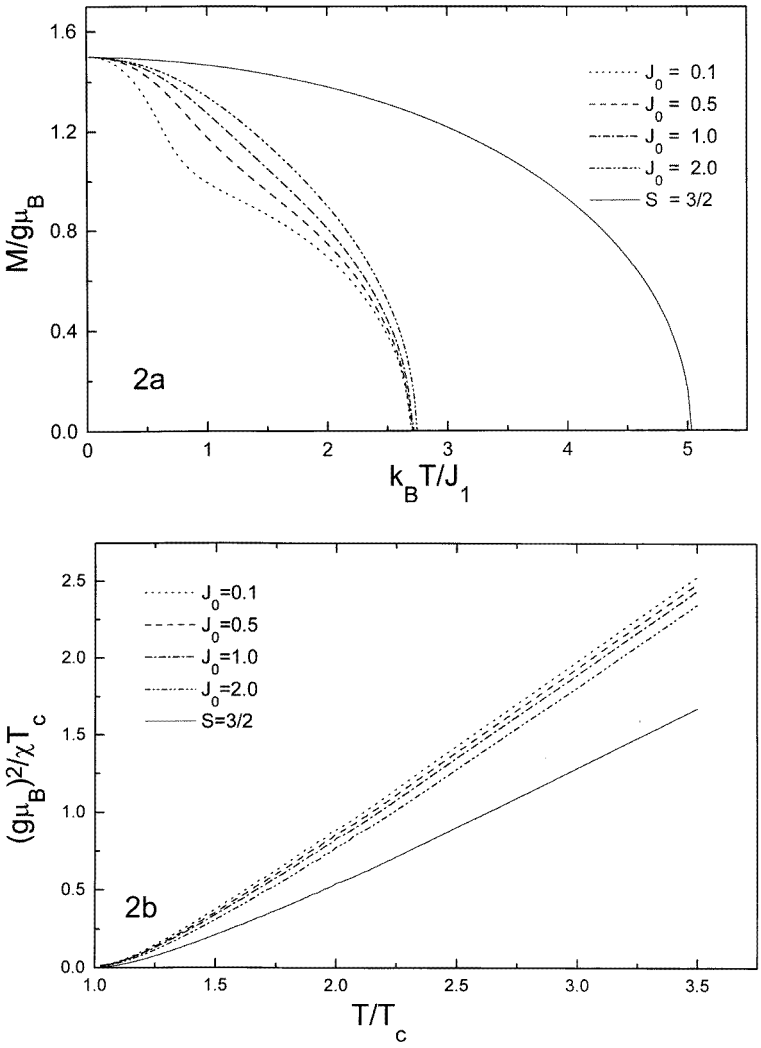

Figure 2. (a) The magnetization and (b) inverse paramagnetic susceptibility as functions of the temperature and J_0. The other parameters are $J_1 = 1.0$, $J_2 = 0.5$, and $J_3 = 0$. The dotted, dashed, chain–dotted, and chain–double-dotted lines refer to $J_0 = 0.1,\ 0.5,\ 1.0,\ 2.0$, respectively. The solid line corresponds to the usual Heisenberg model, with $S = 3/2$ and $J = 1$.

To study the effect of the intra-site spin coupling, we have also calculated the magnetization and paramagnetic susceptibility as functions of temperature for several values

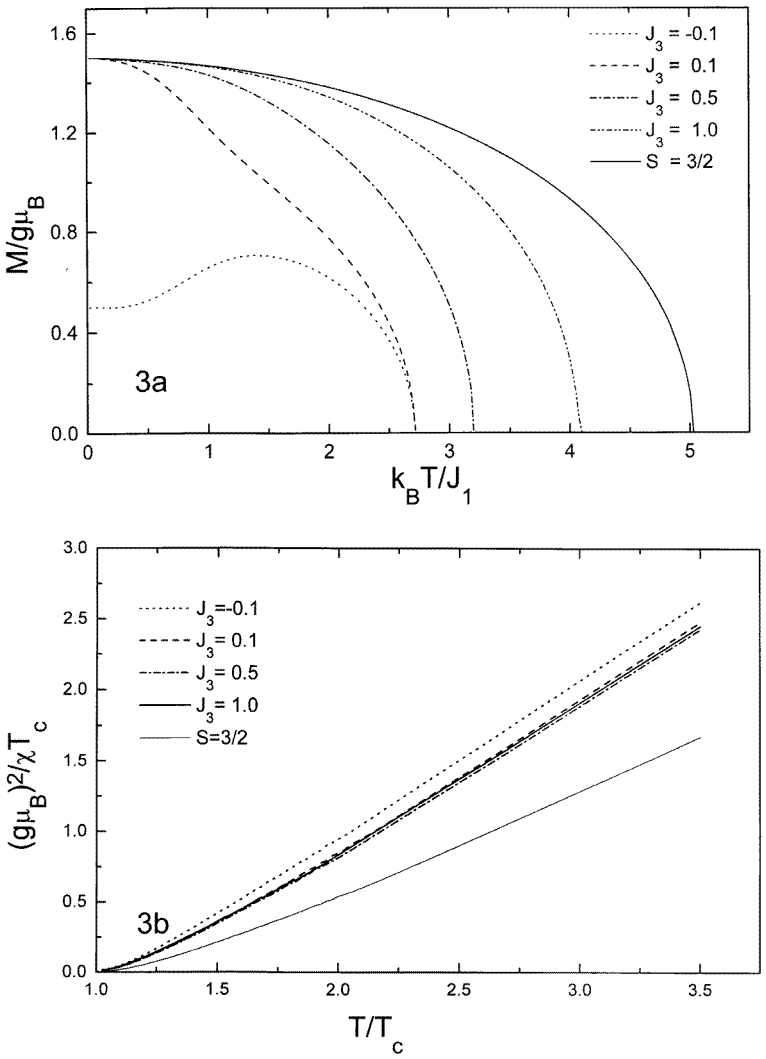

Figure 3. (a) The magnetization and (b) inverse paramagnetic susceptibility as functions of the temperature and J_3. The other parameters are $J_1 = 1.0$, $J_2 = 0.5$, and $J_0 = 0$. The dotted, dashed, chain–dotted, and chain–double-dotted lines refer to $J_3 = -0.1,\ 0.1,\ 0.5,\ 1.0$, respectively. The solid line corresponds to the usual Heisenberg model, with $S = 3/2$ and $J = 1$.

of J_0; the results are presented in figures 2(a) and 2(b). To obtain a clear view of the role played by J_0, we have taken an asymmetrical parameter set, with $J_1 = 1.0$, $J_2 = 0.5$, and $J_3 = 0$. Four different values of $J_0 = 0.1,\ 0.5,\ 1.0,\ 2.0$ correspond to the dotted, dashed, chain–dotted, chain–double-dotted lines. The larger the value of J_0, the stronger the bonding of the two sub-spins. The Curie temperatures do not change much as J_0 is varied, and they are given by $k_B T_C/J_1 = 2.70,\ 2.71,\ 2.72,\ 2.75$ for $J_0 = 0.1,\ 0.5,\ 1.0,\ 2.0$, respectively. The reason that the Curie temperature is so small in comparison with that obtained by the means of the usual Heisenberg model is the fact that $J_3 = 0$, so the highest Curie temperature is determined by J_1 and the effective total atomic spin. At the smallest

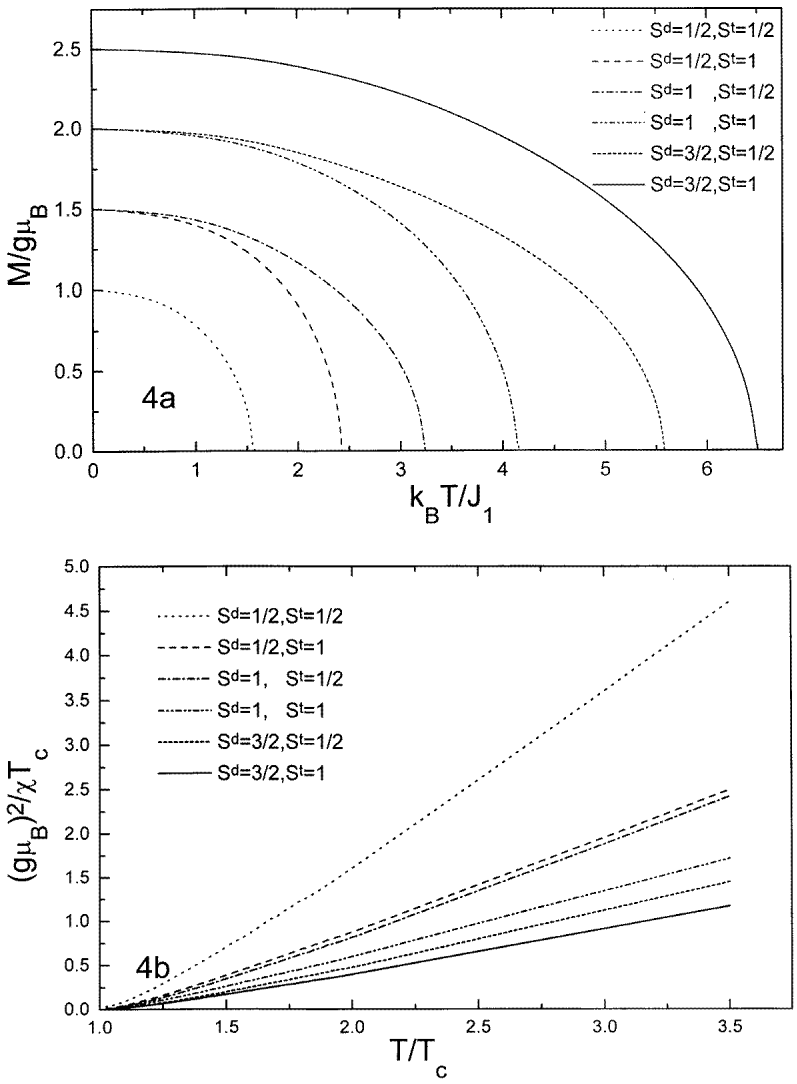

Figure 4. (a) The magnetization and (b) inverse paramagnetic susceptibility as functions of the temperature and sub-spin values. The other parameters are $J_1 = 1.0$, $J_2 = 0.5$, $J_3 = 0.5$, and $J_0 = 0.1$. The dotted, dashed, chain–dotted, chain–double-dotted, short-dashed, and solid lines correspond to $S^d = 1/2$ and $S^t = 1/2$, $S^d = 1/2$ and $S^t = 1$, $S^d = 1$ and $S^t = 1/2$, $S^d = 1$ and $S^t = 1$, $S^d = 3/2$ and $S^t = 1/2$, and $S^d = 3/2$ and $S^t = 1$, respectively.

value of J_0 studied, namely $J_0 = 0.1$, the two sub-spin species are almost decoupled, and the magnetization curve can be viewed as resulting from two sub-spin magnetization curves with different Curie temperatures. The effect of J_0 on the high-temperature paramagnetic susceptibility is the same as in figure 1(b).

The relative sub-spin fluctuations depend on both the intra-site spin coupling and the neighbouring inter-site spin coupling. The effects of the inter-site spin couplings J_3 are demonstrated in figures 3(a) and 3(b), As before, we take the parameters $J_1 = 1.0$, $J_2 = 0.5$, and $J_0 = 0$ as fixed, and let J_3 vary. The dotted, dashed, chain–dotted, and chain–double-

dotted lines correspond the values of $J_3 = -0.1,\ 0.1,\ 0.5,\ 1.0$, and the Curie temperatures are $k_B T_C/J_1 = 2.72,\ 2.72,\ 3.20,\ 4.10$, respectively. Again the solid line refers to the result obtained by means of usual Heisenberg model. One can see a clear difference between the roles played by J_3 and J_0. J_3 bonds the two neighbouring sub-spins, and thus contributes to the build-up of the magnetic long-range order. J_0 only bonds the two intra-site spins, and merely makes full use of the sub-spin exchange energy. Thus, a larger value of J_3 means a stronger binding, and a higher Curie temperature. When J_3 becomes very large, the temperature-dependent magnetization curve approaches that of the usual Heisenberg model. This suggests that large J_3 suppresses the internal spin fluctuations; it makes the two sub-spins behave as a rigid spin which is described by the usual Heisenberg model. Note that the saturation magnetization depends sensitively on the sign of the exchange energy J_3. The two sub-spin moments add when $J_3 > 0$ and oppose each other when $J_3 < 0$. In contrast to the magnetic property below the transition temperature, the influence of J_3 on the paramagnetic susceptibility is weak. The ultimate behaviour is determined by the two sub-spin species independently.

As we can see from the above figures, the magnetic properties of the two-spins-per-site Heisenberg model are quite different from those of the usual Heisenberg model. In figures 4(a) and 4(b), we show the temperature-dependent magnetization and paramagnetic susceptibility for various sub-spin values; the exchange energies are fixed at $J_1 = 1.0$, $J_2 = 0.5$, $J_3 = 0.5$, and $J_0 = 0.1$. In this figure, the dotted, dashed, chain–dotted, chain–double-dotted, short-dashed, and solid lines correspond to $S^d = 1/2$ and $S^t = 1/2$, $S^d = 1/2$ and $S^t = 1$, $S^d = 1$ and $S^t = 1/2$, $S^d = 1$ and $S^t = 1$, $S^d = 3/2$ and $S^t = 1/2$, and $S^d = 3/2$ and $S^t = 1$, respectively. The Curie temperature increases monotonically with the total atomic spin. For the same total atomic spins, the Curie temperatures have different values, because of the asymmetry of the two sub-spin species. It is clear from figure 4(b) that the slope of the paramagnetic susceptibility depends only on the sum of the sub-spin squares.

Table 1. The dependence of the saturated magnetic moment M_s, Curie constant C, and Curie temperature T_C as functions of the exchange energies and sub-spin values.

J_1	J_2	J_3	J_0	S^d	S^t	$M_s/g\mu_B$	$C/(g\mu_B)^2$	T_C
1.00	−0.10	0.25	0.00	1	1/2	1.5	0.913	2.80
1.00	0.10	0.25	0.00	1	1/2	1.5	0.916	2.81
1.00	0.50	0.25	0.00	1	1/2	1.5	0.921	2.85
1.00	1.00	0.25	0.00	1	1/2	1.5	0.927	2.93
1.00	0.50	0.00	0.10	1	1/2	1.5	0.910	2.70
1.00	0.50	0.00	0.50	1	1/2	1.5	0.915	2.71
1.00	0.50	0.00	1.00	1	1/2	1.5	0.920	2.72
1.00	0.50	0.00	2.00	1	1/2	1.5	0.932	2.75
1.00	0.50	−0.10	0.00	1	1/2	0.5	0.903	2.72
1.00	0.50	0.10	0.00	1	1/2	1.5	0.915	2.72
1.00	0.50	0.50	0.00	1	1/2	1.5	0.926	3.20
1.00	0.50	1.00	0.00	1	1/2	1.5	0.927	4.10
1.00	0.50	0.50	0.10	1/2	1/2	1.0	0.502	1.58
1.00	0.50	0.50	0.10	1/2	1	1.5	0.922	2.43
1.00	0.50	0.50	0.10	1	1/2	1.5	0.926	3.24
1.00	0.50	0.50	0.10	1	1	2.0	1.338	4.16
1.00	0.50	0.50	0.10	3/2	1/2	2.0	1.526	5.58
1.00	0.50	0.50	0.10	3/2	1	2.5	1.931	6.50

The above study suggests that the magnetization of our model is a sensitive function of the exchange energies; its saturated magnetic moment is mainly determined by the exchange energies J_0 and J_3, while the Curie temperature depends on both the exchange energies of the same sub-spin species J_1 and J_2 and those of the different sub-spin species J_0 and J_3. The former determines the effective exchange energy of the neighbouring atomic spin, and the latter determines the effective atomic spin value. For temperature much higher than the Curie temperature, the sub-spins are effectively decoupled by the thermal fluctuations, and the Curie constant is just the sum of the contributions from the two sub-spin species, and is independent of the interaction details. The influence of various exchange energies and sub-spin values on the magnetic property is clearly shown in table 1. Note that for the same set of sub-spins, the saturation magnetization depends on the sign of the exchange energy J_3.

Although the results that we obtained in this paper are valid only for localized moments, such as those in the magnetic insulator, we feel that some of the conclusions can also be applied qualitatively to transition metal ferromagnetism. As we discussed in the introduction, the magnetic moment inferred from the Curie constant μ_{eff} and the saturated magnetic moment $\bar{\mu}$ should be the same if the moment is rigid and localized. However, the experimental values are $\mu_{eff} = 3.13\mu_B$ and $\bar{\mu} = 1.91\mu_B$ for iron, and $\mu_{eff} = 1.6\mu_B$ and $\bar{\mu} = 0.6\mu_B$ for nickel, according to a Rhodes–Wohlfarth plot [16]. While part of the difference between μ_{eff} and $\bar{\mu}$ can be explained by the itinerant nature of these systems as was pointed out in an electronic band calculation including the localized moment [17], the Curie constant is still too small in comparison with experimental values. These data indicate that the internal spin fluctuations within an atom should be handled more carefully.

4. Conclusion

In summary, we have studied the magnetic properties of an extended Heisenberg model with two coupled spins per site. The two-spin Heisenberg model is solved using the double-time Green's function method. Our result shows that the saturated magnetic moment depends on the sum of the two sub-spins and their relative orientation, while the Curie constant depends only on the magnitudes of individual sub-spin species. Thus, our result shows that the saturated magnetic moment is not intrinsically related to the Curie constant. Our study also suggests that the discrepancy between the Curie constant and saturated magnetic moment found in some itinerant systems may result from the neglect of some internal spin fluctuations.

Acknowledgments

We would like to acknowledge partial financial support from the National Natural Science Foundation of China and the Education Commission of China.

References

[1] Heisenberg W 1928 *Z. Phys.* **49** 619
[2] Opechowski W 1937 *Physica* **IV** 181
[3] Baker G 1967 *Phys. Rev.* **164** 800
[4] Dyson F 1956 *Phys. Rev.* **102** 1230
[5] Tahir-Kheli R and ter Haar D 1962 *Phys. Rev.* **127** 88
[6] Callen H B 1963 *Phys. Rev.* **130** 890

[7] Domb C and Green M S (ed) 1976 *Phase Transitions and Critical Phenomena* vol 5B (New York: Academic) p 259
[8] Edwards D M 1980 *J. Magn. Magn. Mater.* **15–18** 262
[9] Shastry B S, Edwards D M and Young A P 1981 *J. Phys. C: Solid State Phys.* **14** L665
[10] Reinehr E E and Figueiredo W 1995 *Phys. Rev.* B **52** 310 and references therein
[11] Van Vleck J H 1953 *Rev. Mod. Phys.* **25** 220
[12] Inagaki S 1975 *J. Phys. Soc. Japan* **39** 595
[13] Takano F and Uchinami M 1976 *J. Phys. Soc. Japan* **40** 1305
[14] Kugel K I and Khomskii D I 1978 *Sov. Phys.–Solid State* **20** 1536
[15] Uimin G V 1970 *JETP Lett.* **12** 225
[16] Rhodes P R and Wohlfarth E P 1963 *Proc. R. Soc.* **273** 247
[17] Staunton J B and Gyorffy B L 1992 *Phys. Rev. Lett.* **69** 371